Adaptive data distribution technique for enhancing MB-OFDM UWB link performance in detect and avoid environments

Ahmad M. Rateb*, S.K. Syed Yusof and Norsheila Fisal

Telecommunication Research Group (TRG),
Faculty of Electrical Engineering (FKE),
Universiti Teknologi Malaysia (UTM),
Skudai, 81310 Johor, Malaysia
E-mail: ahmadmrateb@ieee.org
E-mail: kamilah@fke.utm.my
E-mail: sheila@fke.utm.my
*Corresponding author

Abstract: Detect-and-avoid (DAA) mechanisms were developed to minimise potential interference caused by ultra wideband (UWB) systems to in-band active narrowband links. Interference is reduced by minimising emitted power in overlapping bands to create a spectral notch, which provides a certain level of isolation between both systems. Although it has been proved that this procedure deteriorates UWB link performance significantly, no research suggested any scheme to mitigate it. In this paper, we introduce the adaptive data distribution (ADD) technique, which we developed to enhance UWB link performance upon employment of DAA. ADD technique is confined to the physical layer and is fully transparent to the MAC sub-layer. Results have shown a significant reduction in error rates that could provide an SNR gain of at least 4 dB for most covered scenarios. In addition, ADD technique renders performance less sensitive to transmission mode variation and augments its coexistence capability by enabling a UWB device to safely notch 16−55% of its bandwidth.

Keywords: ultra wideband; UWB; detect-and-avoid; DAA; multi-band OFDM; MB-OFDM; WiMedia; ECMA-368; coexistence; spectrum shaping.

Reference to this paper should be made as follows: Rateb, A.M., Syed Yusof, S.K. and Fisal, N. (2011) 'Adaptive data distribution technique for enhancing MB-OFDM UWB link performance in detect and avoid environments', *Int. J. Ultra Wideband Communications and Systems*, Vol. 2, No. 1, pp.1–13.

Biographical notes: Ahmad M. Rateb obtained his BSc in Electronic and Telecommunication Engineering from Ain Shams University, Cairo, Egypt, in 2007. He received his MEng. in 2009 from Universiti Teknologi Malaysia (UTM). Currently, he is doing research for the Telecommunication Research Group (TRG) in UTM. His research interest covers UWB systems, cognitive radio technology and adaptive modulation and coding (AMC).

S. K. Syed Yusof obtained her BSc (cum laude) from George Washington University, USA in 1988 and her MEE and PhD in Electrical Engineering from UTM in 1994 and 2006 respectively. Currently, she is a Senior Lecturer at UTM where she has been there since 1988. Her current research interests are in the field of cognitive radio, UWB, resource allocation and OFDM-based systems.

Norsheila Fisal obtained her BSc in Electronic Communication from the University of Salford, Manchester, UK in 1984 and her MSc in Telecommunication Technology and PhD in Data Communication from the University of Aston, Birmingham, UK in 1986 and 1993, respectively. Currently, she is a Professor with the Faculty of Electrical Engineering, UTM and head of TRG.

1 Introduction

Ultra wideband (UWB) technology has drawn much attention lately, due to its capability of carrying very high data rates over short ranges with transmitted power low enough to be considered as 'background noise' to other systems. The idea of UWB signals goes back the 1960s, it emerged as a way of transmitting voice over a carrier-less wave by sending a series of very short duration impulses, which in return have very wide bandwidth (Ross, 1973). This technology was called impulse radio, and tried to transmit baseband signals right away without the need to modulate them. Conversely, today's UWB only does not

have anything in common with this technology, except the very wide bandwidth they employ.

Modern UWB concept was born on February 14, 2002 when the Federal Communications Commission (FCC) of the USA approved a spectrum in the range 3.1–10.6 GHz to be available for unlicensed use of UWB signals. The FCC defined a UWB signal as one that either (FCC, 2002):

- occupies at least 500 MHz of spectrum
- has a 10 dB bandwidth greater than or equal to 20% of its centre frequency.

In addition, the FCC required that a UWB signal must abide to a spectral mask that confines its in-band transmitted power density to −41.3 dBm/MHz. Later on, regulatory bodies from other countries such as Japan and the European Union followed the FCC's path and issued similar UWB allocations (Ahmed and Ramon, 2009).

The enormous band allocated for UWB operation necessarily overlaps with bands allocated to various wireless systems such as WiFi (IEEE 802.l1a), WiMax, UMTS, satellite communication and other governmental communication systems (Ely et al., 2004; Duranti et al., 2006). Thus, UWB has to coexist peacefully with various incumbent and future active *narrowband* systems – as compared to UWB's bandwidth − sharing the same band of operation. Despite the very low power constraint on UWB emissions, this coexistence issue and its potential effect on narrowband systems have witnessed a debate between UWB technology promoters and regulatory bodies all over the world. It is possible that a low power UWB radio operating in close proximity to a narrowband receiver could raise its noise floor by an amount sufficient to affect the performance of the narrowband receiver (Chiani and Giorgetti, 2009). Modern wireless technologies are adaptive in nature and a loss in performance observed at the receiver will probably cause the transmitter to fall back to a more robust modulation scheme with lower overall throughput, or to step up the transmit power to maintain the overall system performance. Several studies have proved that the presence of an active UWB device at a short distance from a narrowband link has the potential of causing interference in the overlapping bands (Rahim et al., 2007; Chiani and Giorgetti, 2009); while others showed that a UWB device is affected as well by interference from narrowband signals (Shi et al., 2007; Snow et al., 2007).

In order to release regulatory concerns about UWB interference to narrowband systems, *detect-and-avoid* (*DAA*) mechanism (Mishra et al., 2007a) was proposed as an approach to minimise any possible interference caused by UWB to narrowband users in compromise to its complexity and performance. DAA operates by periodically *detecting* the presence of active in-band narrowband links and acting to *avoid* these links by reducing its transmitted power over the overlapping bands, thus creating a spectral *notch*. Accordingly, DAA technology provides the flexibility needed to enable universal support of regulatory measures, and relax concerns about interference. DAA was adopted and required by regulatory bodies in many countries such as the EU, Japan and Korea (Commission of the European Communities, 2007; MIC, 2005; Kim et al., 2008). However, the advantage of DAA comes at the price of degraded UWB performance (Mishra et al., 2007a, 2007b; Rateb et al., 2008, 2010). Table 1 lists the frequency bands that require DAA in various countries (WiMedia Alliance, 2009).

Table 1 Frequency bands requiring DAA in different countries

Country	*Bands (MHz)*	*Band #*
European Union	3,168−4,752	1, 2, 3 and 11
	8,448−8,976	
Korea	3,168−4,752	1, 2 and 3
Japan	3,696−4,752	2 and 3
China	4,224−4,752	3

Several studies focused on enhancing the capabilities of narrowband link detection in UWB, and increasing isolation in overlapping bands (Yamaguchi, 2004; Chiang and Lansford, 2005; Clancy and Walker, 2006). On the other hand, only Mishra et al. (2007a, 2007b) considered the effect of DAA on UWB link performance. This study was limited in channel model, data rates and covered cases, as pointed out by the authors. Furthermore, no research proposed methods or techniques to alleviate this effect. Channel coding was considered as the sole recovery mechanism for any possible loss of UWB data resulting from spectral shaping. However, in the same article, channel coding was unable to recover data loss at data rate of 480 Mb/s, as redundancy allocated for channel coding is reduced to gain more data throughput.

Since UWB is expected to coexist with various narrowband systems with different natures, frequency bands, power, and bandwidth; therefore, the transmitted spectral shapes dictated by DAA tend to be random. This would render UWB performance unpredictable, and directly impacts its reliability, as performance lower bound cannot be guaranteed. Typically, in such a scenario, a UWB device would first attempt to reduce data transmission rate aiming to reach an acceptable performance level. If performance requirement was still unsatisfied, a UWB device may drop the whole band and attempt transmission over other bands. While UWB is designed to support QoS-enabled services, DAA imposes a serious threat to the integrity of its operation, which translates into a frustrating user experience.

In this paper, we propose an effective technique which we call *adaptive data distribution* (ADD) technique that helps mitigating the harmful effect of DAA on UWB link performance and enables it to sustain a satisfactory level of reliability. This technique is designed to work at the UWB physical layer with full transparency to the MAC sub-layer. At the same time, it implies minimum modification to the high rate UWB working standard specifications (ECMA International, 2008). The main contribution of this paper is twofold. Firstly, the proposed technique enables a UWB

device undergoing DAA mechanism to coexist with larger number of narrowband users by enabling it to notch a larger portion of its bandwidth with minimal effect on performance while sustaining its data rate. Secondly, the proposed technique is based on a novel channel coding scheme called *hybrid rate coding* (HRC) scheme, which provides a highly flexible range of arbitrary rational channel coding rates, without imposing a significant increase in complexity. This scheme can be used in other systems and for other purposes, such as increasing bandwidth efficiency (Rateb et al., 2009).

The remainder of this paper is organised as follows: we provide a brief summary of the current UWB standard for high data rates in Section 2. Section 3 discusses the DAA mechanism and its stages. We explain our proposed technique in detail in Section 4, including the novel coding scheme it employs and its theoretical performance. Section 5 proves the effectiveness of the proposed technique through simulated results and discussions. Finally, concluding remarks are given in Section 6.

2 Overview on ECMA-368 specifications

Currently, the de-facto standard for high data rate UWB is the ECMA-368 standard (ECMA International, 2008) developed by the WiMedia Alliance. The ECMA-368 standard is supported by a powerful coalition of industry giants such as Intel, Nokia, NEC, Samsung, NXP/Philips, etc. Its physical layer is based on multiband orthogonal frequency division multiplexing (MB-OFDM) (Batra et al., 2004), which relies on the successful OFDM technology. It supports physical data rates up to 480 Mb/s, which can support a wide range of high rate WPAN applications. It also supports quality of service (QoS) through pre-reservation of time slots within a time division multiple access (TDMA) framework. The standard has been selected for two major application technologies: certified wireless universal serial bus (CW-USB), which shall replace the conventional wired USB, and the third generation of Bluetooth (Bluetooth 3.0).

Figure 1 MB-OFDM band plan

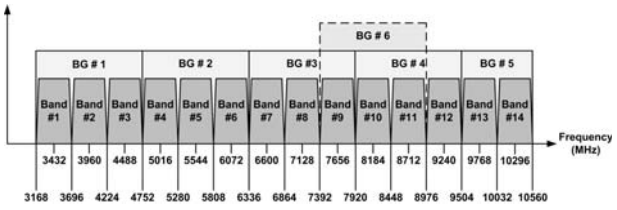

In MB-OFDM, the spectrum of 7.5 GHz from 3.1 GHz to 10.6 GHz is divided into 14 bands of 528 MHz each. As elaborated in Figure 1, the 14 bands are grouped into six band groups (BGs), where each band group comprises three bands except for the BG #5 which comprises only two. Transmission takes place over one of the available BGs. A device undergoes frequency hopping between the centre-frequencies of the bands comprised in the BG. Frequency is switched after each OFDM symbol. This operation is controlled by a predefined time-frequency code (TFC). The standard defines ten different TFCs for each BG, and classifies them into three modes, according to the number of bands employed for hopping (1 or 2 or 3).

WiMedia transceiver is essentially a conventional OFDM transceiver that uses a total of 128 OFDM subcarriers divided into 100 data subcarriers, 12 pilot subcarriers, ten guard subcarriers, and six unused subcarriers. MB-OFDM uses quadrature phase shift keying (QPSK) modulation in low data rates, and dual carrier modulation (DCM) in high data rates (Batra and Balakrishnan, 2006) as shown in Table 2. DCM introduces additional redundancy by mapping 4 bits onto two 16-point constellations. The symbols from the two constellations are then mapped onto tones that are separated by at least 200 MHz in bandwidth.

Table 2 Physical layer data rate-dependent parameters

Data rate (Mb/s)	*Spreading*	*Code rate*	*Spreading factor*
53.3	TDS+FDS	1/3	4
80		1/2	4
106.7	TDS	1/3	2
160		1/2	2
200		5/8	2
320	None	1/2	1
400		5/8	1
480		3/4	

The standard supports a set of four convolutional code rates which are: 1/3, 1/2, 5/8 and 3/4. The last three code rates are generated from the mother rate 1/3 by employing code puncturing. For improved performance over fading channel conditions, the standard also supports frequency domain spreading (FDS) and time domain spreading (TDS) for certain data rates. In FDS, the same data symbol is transmitted twice over two widely separated subcarriers in the same OFDM symbol; whereas in TDS, the same OFDM symbol is transmitted twice on two consecutive time slots. The combination of spreading with available code rates generates a set of eight data rates, as listed in Table 2.

According to the standard MAC specifications, the main timing unit is the *superframe*, which is made up of 256 time slots called Medium Access Slots (MASs) of 256 μs each. Medium access is provided within a distributed reservation protocol (DRP) − a form of TDMA − which allows each device to reserve a set of slots in advance, according to its application requirements. The reservation process prevents competition among devices for medium access and therefore reduces the overall MAC overhead. As a result, MAC-level data throughput is increased (Liu et al., 2009). The reservation also allows for guaranteed service to applications that require it, such as streaming video/audio.

To allow for coordination of devices in the network, each device is expected to send a beacon frame every superframe. Beacons are special packets that carry most of

the control information necessary for the distributed network to exist and to be stable. They also carry information about channel reservations that each device makes. MAC clients can also send their layer's control information in the beacons in the form of *information elements* (*IE's*). Notice that beacons are overlain on MASs at the beginning of each superframe. Since beacons carry very critical information, they are always transmitted over the lowest (and most robust) data rate of 53.3 Mb/s in order to maximise the probability that information carried on beacons is received correctly. Moreover, each beacon payload is accompanied with a 4 bytes frame check sequence (FCS) to detect errors. If error is detected, beacon retransmission is requested within an automatic repeat request (ARQ) protocol.

The standard supports transmitted spectrum shaping for avoidance of other narrowband users allocated within the UWB band in order to comply with DAA requirements. This was added in the 2nd edition of the standard. The transmitted signal is sent in the context of a tone nulling array (TN array) of 384 elements. These elements correspond to the total number of OFDM tones (subcarriers) of the BG used for transmission. TN {0−127} apply to the tones of the lowest frequency band in the current band group, TN {128−255} to the middle band, and TN {256−383} to the highest band. Each tone nulling element can take the values of 0 or 1; if the value is 0, then the transmitter should take steps to minimise the transmitted signal power at the frequency of the corresponding tone; if the value is 1, then the signal is unaffected by tone nulling. Figure 2 illustrates how TN array is mapped on OFDM tones to create a notch in the transmitted spectrum.

Figure 2 Mapping of TN array on OFDM tones (see online version for colours)

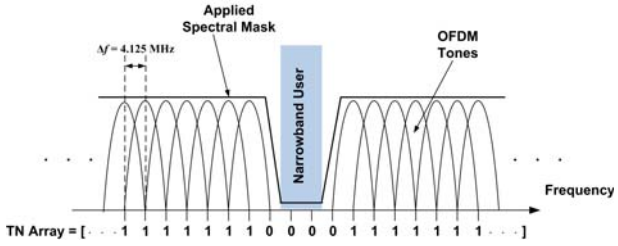

3 DAA mechanism

In this section, we provide a brief explanation of the stages involved in the DAA mechanism operation. Figure 3 describes the main stages of the DAA mechanism, which can be summarised into three stages in the context of the WiMedia UWB physical layer characteristics:

1 spectral analysis of the surrounding medium to detect the presence of active narrowband links (*detect stage*)

2 informing the receiver of the transmitted spectrum shape

3 adaptive spectral shaping (*avoid stage*) to minimise interference at overlapping bands.

Figure 3 Block diagram showing simplified DAA operation at the transmitter and receiver

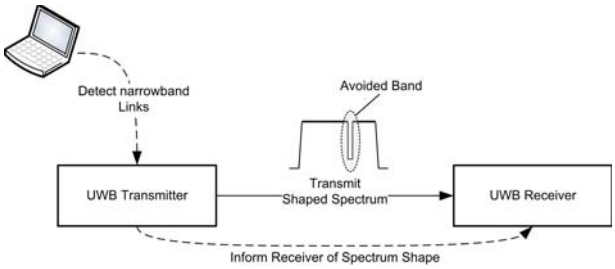

3.1 Detect stage

By using the inherent FFT engine in all OFDM transceivers, the UWB device can act as a spectrum analyser, with resolution of 4.125 MHz (528 MHz BW/128 points FFT) (Batra et al., 2006). The average power levels transmitted by other NB devices within the active UWB bands can be measured by averaging the received signal over time. Measured power levels of detected links that require an *avoid* action should exceed a certain threshold that indicates possible interference hazard. Threshold values vary depending on each county's regulations and the avoided narrowband system. Generally, protection of the narrowband link requires that the UWB interference is equal to thermal noise floor. The thermal noise power per MHz can be calculated as:

$$N = kTB_n = -114\ dBm/MHz \tag{1}$$

where k = Boltzmann's constant (1.38×10^{-23} J/K), $T = 290$ K is the system temperature, and B_n = 1 MHz is the system bandwidth. Assuming 0 dB*i* antenna gain, UWB interference can be represented as:

$$I_{UWB} = P_{UWB} - (L + S) \tag{2}$$

where P_{UWB} is the transmitted power spectral density of the UWB device and equals −41.3 dBm/MHz, L represents the path loss, and S represents losses due to shadowing. Equating (1) with (2) yields:

$$N = P_{UWB} - (L + S) \tag{3}$$

$$L + S = P_{UWB} - N = -41.3 - (-114) \approx 73\ dB \tag{4}$$

The LHS of (4) represents minimum loss due to channel that makes UWB interference below noise floor. Consequently, detection threshold is specified as

$$P_{th} = P_{NB} - (L + S) = P_{NB} - 73 \quad dBm/MHz \tag{5}$$

This threshold value does not incorporate losses due to multipath and other effects, which may further reduce it by about 20 dB (Mishra et al., 2007a). Detection using this approach is usually called '*energy detection approach*'. Yet,

Mishra et al. (2007a) showed that energy detection suffers a large probability of false alarm (probability of falsely detecting a nonexistent NB link) due to spurs usually found in the measured power-spectrum profile that result from carrier leakage, I/Q imbalance and other reasons. However, this is the simplest and most cost-effective approach available.

Other approaches involve detecting specific features of the targeted NB signal. For example, for detecting WiMax, the specific feature could be its packet preamble (Tang, 2005). This minimises the probability of false alarm since detection is based on signal type, not energy. However, in order to be able to detect all kinds of potential NB links, this would require a library of system features that may vary in different countries, and need to be updated to support new systems. This renders such an approach difficult to implement. This approach is usually called '*signal type detection*' or '*coherent detection*'.

3.2 Informing receiver of transmitted spectrum shape

According to Mishra et al. (2007a), the UWB receiver may be either *aware* or *unaware* of the transmitted spectrum shape (which tones are active, and which are not). If the receiver is aware of the spectrum shape, it may use this knowledge to improve its link performance, e.g., using erasure marking (Li et al., 2003; Snow et al., 2006). In the second case, the receiver tries to reconstruct information lost solely by exploiting the redundancy due to channel coding.

Referring to the current ECMA-368 specifications, the receiver can be aware of the transmitted spectrum shape. A device that intend to null one or more tones during its transmissions includes a *tone-nulling information element* (TN IE) in its beacon. The TN IE is used to announce which physical layer tones are not used (nulled) when transmitting frames from this device. This will make all other devices in the surrounding range (potential receivers) aware of the shape of the transmitted signal for this device, and which tones will be used for data transmission. Typically, the transmitted power at these tones should adhere to the limits set by regulations.

3.3 Avoid stage

When narrowband link protection is needed at certain bands, interference can be avoided by several methods. Switching to a different BG or changing the hopping pattern may solve the problem. However, it tends to be impractical if the number of UWB users or detected narrowband links increases. Optimally, the UWB signal strength needs to be lowered just at the frequency where protection is needed; in other words, create a notch in the overlapping band by dropping (nulling) respective OFDM tones. This form of spectral shaping by nulling of tones is feasible using existing UWB chips and devices (Batra et al., 2006), since it can be done via an all-digital operation (no analogue filtering required).

Figure 4 shows the transmitted baseband spectrum shape for ten nulled tones (notch width of 41.25 MHz), resulting in a notch depth of about 15 dB. Most worldwide regulations require that a device undergoing DAA should reduce power to less than −70 dBm/MHz in victim bands (MIC, 2005; Kim et al., 2008). Hence, at least 29 dB (−70 + 41.3) notch is required. Nulling more tones on both sides of the notch can yield larger depth; however, Mishra et al. (2007b) showed that even with 40 nulled tones, the required notch depth could not be achieved. Various methods have been proposed to increase notch depth such as active interference cancellation (Brandes et al., 2005) and applying a digital notch filter in time domain post IFFT (Mishra et al., 2007a). However, all this work still entails that data transmitted on the notched band is lost as the applied notch makes it impossible for the receiver to detect any transmitted signals on that band.

Figure 4 Transmitted baseband UWB spectrum shape with ten nulled tones

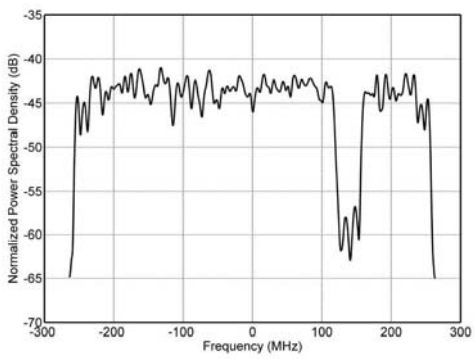

After the OFDM waveform is synthesised in the frequency domain, and after spreading, pilot and guard insertion are complete; the transmitter applies the TN array it generated during detection stage. Typically, the transmitter replaces data on tones corresponding to a '0' in the TN array by a stream of zeros, as shown in Figure 5 (or apply digital notch filter or any other approach). This creates a notch in the transmitted signal spectrum at the required band.

Figure 5 WiMedia OFDM transmitter applying tone nulling

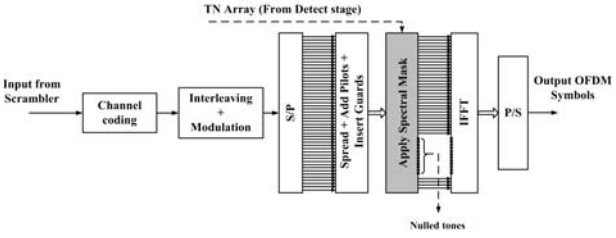

At the receiver, redundancy provided by FDS, TDS, and channel coding is basically exploited to recover data loss. Mishra et al. (2007a) examined the packet error rate (PER) performance for 13 and 21 nulled tones at data rates of 53.3, 200 and 480 Mb/s. The simulations were performed in non-frequency hopped mode for a multipath channel of delay spread of 20 ns. The target PER of 8% required by the

standard could be reached for 53.3 and 200 Mb/s (with lowered link margins). However, for 480 Mb/s, the target PER could not be reached for any transmit power, and the link suffered complete failure. Hence, the performance of a UWB link operating in a DAA-required band is highly compromised, especially for high data rates, which are the least robust and the most desirable for consumers. Consequently, it is vital to come up with a method that enables a UWB device to host a DAA mechanism more effectively, in order to attain link reliability and bandwidth efficiency.

4 Methodology

In this section, we introduce our methodology for preventing loss of transmitted data due to tone nulling. We developed a technique which we term as '*adaptive data distribution* (ADD)' technique, since its main task is to distribute payload data on active tones in a manner that avoids data transmission on nulled tones. As we are concerned with the practical impact of our work, we set the following restrictions during formulating our method:

- *minimum modification to physical layer architecture*: in order to comply with the standard specifications
- *transparency to MAC sub-layer*: our technique has to operate autonomously without any aid or supervision from the MAC sub-layer
- *sustaining data rate*: in order to satisfy the requirements of applications running on upper layers
- *minimum added complexity*: to keep cost and power consumption as low as possible.

4.1 ADD technique

The reason for degraded performance of UWB link upon nulling OFDM tones in the avoided bands is that all symbols transmitted over these tones are not detected by the receiver, which results in losing a certain portion of transmitted data. Snow et al. (2006) suggested marking all symbols received on avoided bands as erasures, which implies that the Viterbi decoder is not going to consider them (or deals with them as less reliable information) for branch metric calculation, thus preventing them from 'misleading' the decoder. However, the presence of a large number of erasures with random locations deteriorates the performance of the decoder and may lead to catastrophic decoding.

According to our point of view, the problem may be solved if we adaptively ceased transmission of data on these tones, and use only the remaining active (not-nulled) tones for transmission. This implies that the effective bandwidth used for transmission is reduced by a certain ratio, and hence the overall data rate. However, as the MAC sub-layer supports only a limited set of data rates, it is necessary to keep data rate unchanged in order to sustain transparency to MAC.

To maintain data rate, we have to transmit the same number of information bits per packet within a reduced number of channel-coded bits that can be carried on the remaining active tones. In other words, ADD has compensate for the reduced number of data-carrying OFDM tones by re-adjusting channel coding rate respectively, in a manner that keeps data rate unchanged. Figure 6 compares conventional operation of DAA to that employs ADD. As ADD avoids transmission over notched (avoided) bands, consequent loss of data can be prevented. Hence, ADD can provide substantial gains in performance especially for large number of nulled tones and high data rates, as we will show in Section 5.

Figure 6 Schematic diagram comparing conventional DAA operation to that employing ADD (see online version for colours)

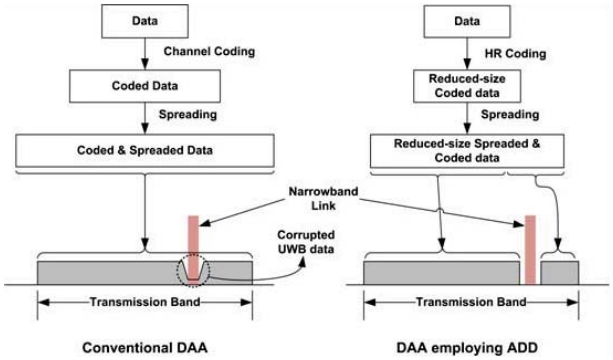

The range of possible code rates that ADD needs starts at the original code rate used by the current data rate c_0 until it reaches the maximum allowed code rate c_{max}. c_{max} is specified according to performance requirements. Table 2 lists all standard data rates with the code rate and spreading each data rate employs. To avoid modifying the standard specifications, we chose c_{max} to be the maximum code rate available in the standard, which is 3/4. This entails that, according to the table, our work cannot be applied to the data rate 480 Mb/s, since it already employs the maximum code rate 3/4. Yet, this can be remedied by adding other puncturing patterns that can generate a larger code rates. However, this is beyond the scope of this paper, since we are mainly concerned here about the integrity of the principle itself.

As explained in Section 2, nulled tones are represented by '0' in the TN array which is formed of 384 elements that correspond to all OFDM tones in the band group. Out of these 384 elements, we are concerned with the 300 data-carrying tones which they comprise (100 for each band). If d tones were required to be nulled, the number of remaining active tones becomes

$$\Omega = 128\lambda - d \tag{6}$$

where λ is the number of bands employed in the BG according to the TFC applied. As d may comprise any combination of data-carrying tones data, pilots, guards and unused tones, then the number of active data-carrying tones remaining to be utilised in transmission is

$$\omega = 100\lambda - \delta \tag{7}$$

where δ is the total number of nulled data-carrying tones within d nulled tones in the bands employed for transmission. Consequently, we can determine the minimum number of active data-carrying tones that ADD can handle by using the following equation:

$$\omega_{\min} = \left\lceil 100\lambda \left(\frac{c_0}{c_{\max}} \right) \right\rceil \tag{8}$$

where $\lceil x \rceil$ stands for the largest integer more than or equal to x. By setting c_{max}=3/4, ADD can enable a UWB device to null 16−55% of its tones, depending current data rate (can be increased if c_{max} was increased). Table 3 lists the maximum possible number of nulled data-carrying tones $\delta_{\max} = 300 - \omega_{\min}$ offered by ADD according to (8).

Table 3 Maximum number of nulled data tones offered by ADD for standard data rates ($\lambda = 3$ and $c_{max} = 3/4$)

Data rate (Mb/s)	c_0	$\delta_{max} = 300 - \omega_{min}$
53.3	1/3	166
80	1/2	100
106.7	1/3	166
160	1/2	100
200	5/8	50
320	1/2	100
400	5/8	50
480	3/4	0

Let K be the number of information bits to be transmitted for each packet payload, and N be the resulting number of coded bits. The number of coded bits for the same number of information bits per code block has to be reduced in order to maintain data rate. Hence, the total number of coded bits that can be carried on ω data tones can be calculated as

$$n = \left(\frac{\omega}{100\lambda} \right) \frac{K}{c_0} = \left(\frac{\omega}{100\lambda} \right) N \tag{9}$$

Thus, we need to encode K bits into n bits only instead of N, which yields a code rate required to be somewhere in between two standard code rates (as long as $\omega \geq \omega_{\min}$).

$$c_x < \left(\frac{K}{n} \right) < c_y \text{ , for } \delta > 0 \tag{10}$$

such that,

$$c_x \geq c_0 \text{ , } c_y \leq c_{\max} \text{ and } \left[c_x, c_y \right] \in \left\{ \tfrac{1}{3}, \tfrac{1}{2}, \tfrac{5}{8}, \tfrac{3}{4} \right\} \tag{11}$$

Obviously, the required code rates for ADD may take rational forms with unconventional values. Such rates can be achieved through applying very long puncturing patterns over large sized blocks of coded bits. However, this is a very complex solution due to the long length of the pattern, and the very large number of simulations needed to find the optimum patterns required, which tends to be impossible. In the next section, we present hybrid-rate coding scheme, which is a simple but yet powerful alternative (Rateb et al., 2008, 2010).

4.2 HRC scheme

For each block of K information bits, let we divide it into two sub-blocks of k_x and k_y bits, and encode them by standard component code rates c_x and c_y, to yield coded sub-blocks of n_x and n_y bits, respectively. Hence, the required code rate can be obtained if,

$$K = k_x + k_y = n_x c_x + n_y c_y \tag{12}$$

such that,

$$n = n_x + n_y \tag{13}$$

From (12) and (13) we can get:

$$k_x = \frac{c_x c_y}{c_y - c_x} \left(n - \frac{K}{c_y} \right) = \gamma n - \frac{c_x}{c_y - c_x} K \tag{14}$$

$$k_y = \frac{c_x c_y}{c_y - c_x} \left(\frac{K}{c_x} - n \right) = \frac{c_y}{c_y - c_x} K - \gamma n \tag{15}$$

where $\gamma = \dfrac{c_x c_y}{c_y - c_x}$.

Figure 7 HRC scheme

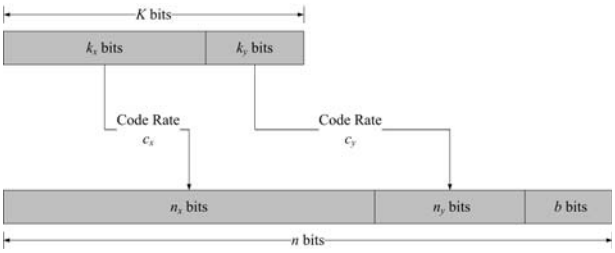

However, from (15), k_x and k_y may not have integer values for all possible number of nulled data tones at all data rates. In order to fix this, we take the largest possible integer values of k_x and k_y, and allow for the insertion of b dummy bits after encoding, such that exactly n encoded bits result from the whole process. We do this by encoding data to yield the largest integer less than n, and then insert the required number of bits as dumb bits at the beginning of the coded block, that are removed before decoding. Inserting dummy bits involves replacing n by $n-b$, which changes (13), (14) and (15) to become

$$n = n_x + n_y + b \tag{16}$$

$$k_x = \gamma \left(n - b \right) - \frac{c_x}{c_y - c_x} K \tag{17}$$

$$k_y = \frac{c_y}{c_y - c_x} K - \gamma \left(n - b \right) \tag{18}$$

Thus, the HRC encoder has to ensure that the term $\gamma \times (n - b)$ always has an integer value by inserting the smallest suitable value of b. Our calculations showed that the term b shall not exceed 3 bits for all code rates ADD might require in any case. The overall idea of HRC is represented in Figure 7.

4.3 HRC at the WiMedia physical layer

As we mentioned earlier, standard code rates are all generated from a single convolutional encoder with rate 1/3 by applying different puncturing patterns. The HRC channel encoding/decoding process within the WiMedia transmitter/receiver is described in Figure 8. HRC coding operates by multiplexing through the outputs of puncturers within each frame payload (K) according to the calculated values of k_x and k_y. The control logic block shown in the figure uses (17) and (18) to generate k_x , k_y and b, which control multiplexing/de-multiplexing operations according to these values. Decoding is the opposite process of the encoding one; the receiver uses the TN IE received within its beacon to extract all the required parameters used in the decoding process. HRC scheme does not impose any additional encoding/decoding complexity, as the only modification it implies on the standard encoder/decoder is how coded data output from the convolutional encoder is punctured at the transmitter, and de-punctured at the receiver. Consequently, the convolutional encoder and Viterbi decoder depicted in Figure 8 are neither affected nor aware of the HRC operation.

Figure 8 Hybrid-rate encoding/decoding at transmitter /receiver

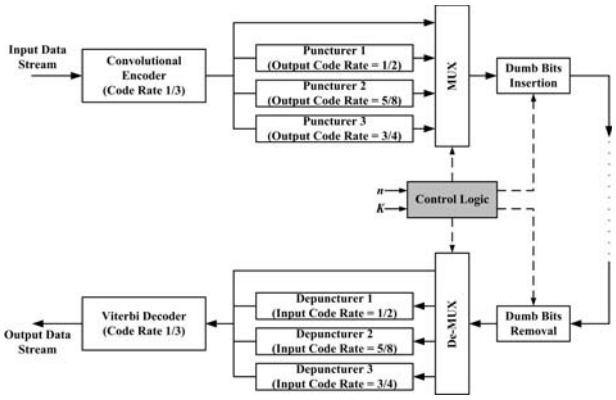

4.4 Theoretical performance of ADD technique

The upper bound of bit error probability for a soft decision convolutionally coded data stream is given by (Proakis, 2001)

$$P = \sum_{d=d_f}^{\infty} e_d P_d \tag{19}$$

where e_d is the sum of bit errors (the information error weight) for error events of distance d; values for e_d at different code rates can be found in (Bocharova and Kudrayashov, 1997) and d_f is the free distance of the code. P_d is the pair-wise error probability, given by

$$P_d = Q\left(\sqrt{2dR_c \frac{E_b}{N_0}}\right) \tag{20}$$

for a QPSK-modulated signal over AWGN channel. Here, R_c represents the code rate, E_b denotes the received energy per information bit, $N_0/2$ is the double-sided power spectral density of the noise process, and $Q(x) = \left(\sqrt{2\pi}\right)^{-1} \int_x^{\infty} e^{-z^2/2} dz$ is the well known Q-function. Thus,

$$P = \sum_{d=d_f}^{\infty} e_d Q\left(\sqrt{2dR_c \frac{E_b}{N_0}}\right) \tag{21}$$

For HRC, two component code rates c_x and c_y are employed to encode sub-blocks of size k_x and k_y, respectively, to yield an overall code rate of $R_c = K/n$. Therefore, for HRC and assuming the number of coded bits per coded block is large enough and they are well interleaved to distribute error events uniformly over sub-blocks, (21) becomes (neglecting b)

$$P_{HR} = \frac{k_x}{K} \sum_{d=d_x}^{\infty} e_d^x Q\left(\sqrt{2d \frac{K}{n} \frac{E_b}{N_0}}\right) + \frac{k_y}{K} \sum_{d=d_y}^{\infty} e_d^y Q\left(\sqrt{2d \frac{K}{n} \frac{E_b}{N_0}}\right) \tag{22}$$

where d_x and d_y are the free distances of code rates c_x and c_y, respectively, K/n is the overall HRC code rate while e_d^x and e_d^y are the sum of bit errors of code rates c_x and c_y, respectively. Equation (22) shows that the error performance of HRC-coded data can be considered as a linear combination between the performance of its two component code rates. It is lower bounded by the performance of the code rate c_x (for $k_x = K$), and upper-bounded by the performance of the code rate c_y (for $k_y = K$).

While applying random or pseudo-random puncturing patterns generated to satisfy the required code rate could do the job of HRC, these patterns are not guaranteed to be optimal and may also be catastrophic. On the other hand, as HRC component code rates are generated using optimum puncturing patterns, the resulting code rate is guaranteed to have maximum distance properties, hence best possible performance.

Figure 9 presents theory vs. simulation results for the performance of two rational value code rates generated by HRC in an AWGN channel with QPSK modulation. Theoretical performance is plotted using equation (22). The code rates have the values of 21/32 (0.65625) and 23/32 (0.71875). Thus, they employ component code rates c_x=5/8 (0.625) and c_y = 3/4 (0.75). The plots show that the simulated results for both code rates follow closely the theoretical curves. The figure also proves that the

performance of both code rates is bounded by the performance of the component code rates, which conforms to (22).

Figure 9 Theoretical HRC performance vs. simulation results for QPSK-modulated signal over AWGN channel

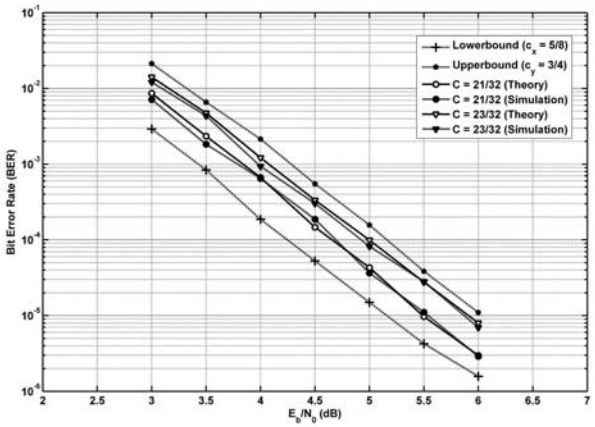

The performance of a UWB link employing ADD can thus be approximated for an AWGN channel, QPSK modulation (no spreading) to be

$$P_{ADD} = \eta P_{HR} \tag{23}$$

where η = 100/128 is the probability that a nulled tone would be a data-carrying tone. Spreading can be accounted for by multiplying the value of E_b/N_0 by the spreading factor. Performance is mainly proportional to P_{HR} as data transmission is now isolated from the tone nulling issue; i.e., performance does not incorporate any losses due to corruption. Using (9) and (22), equation (23) becomes

$$P_{ADD} = \eta \left[\begin{array}{l} \dfrac{k_x}{K} P_x\left(\dfrac{100\lambda}{\omega}\dfrac{E_b}{N_0}c_0\right) \\ + \dfrac{k_y}{K} P_y\left(\dfrac{100\lambda}{\omega}\dfrac{E_b}{N_0}c_0\right) \end{array} \right] \tag{24}$$

such that,

$$P_x(\chi) = \sum_{d=d_x}^{\infty} e_d^x Q\left(\sqrt{2d\frac{K}{N}\chi}\right) \tag{25}$$

and

$$P_y(\chi) = \sum_{d=d_y}^{\infty} e_d^y Q\left(\sqrt{2d\frac{K}{N}\chi}\right) \tag{26}$$

We can thus conclude from (24) that ADD performance is a function of several factors such as ω, E_b/N_0 and original code rate $c_0 = k/N$.

4.4 Operation of ADD in WiMedia physical layer

A block diagram representing overall design and operation of the UWB transmitter and receiver employing DAA with ADD is provided in Figure 10. Shaded blocks represent those related to ADD operation. Comparing this figure to Figure 5, we can see that other than HRC, ADD did not impose any significant modification to the standard physical layer architecture. Besides employing HRC scheme, ADD only changes the way data is distributed on OFDM tones, where data is allocated only to active tones that are correspond to '1' in the TN array, while nulled tones that correspond to '0' are completely ignored. Likewise, only data carried on active tones are considered at the receiver, while nulled tones are discarded. This function is represented by the shaded block located before IFFT stage in the transmitter, and after FFT stage in the receiver, as illustrated in Figure 10.

Figure 10 Block diagram of the baseband WiMedia transmitter and receiver architecture extended to support ADD. Shaded blocks represent those involved in ADD

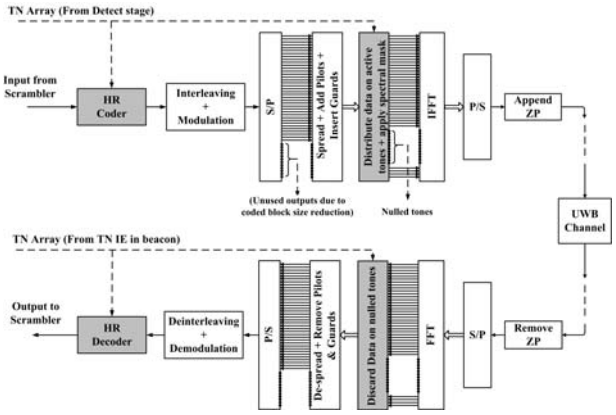

5 Results and discussion

In this Section, we provide physical layer Monte Carlo simulation results to evaluate the performance advantage that ADD provides. The WiMedia standard sets a target value of 8% PER as the physical layer performance criterion (ECMA International, 2008). This PER is measured at a packet size of 1024 octets. We thus provide PER vs. SNR plots that represent different transmission conditions. We focused our attention on high data rates, specifically 200 Mb/s and 400 Mb/s.

5.1 Simulation environment and assumptions

Results are generated from a baseband-equivalent model of the UWB transmitter and receiver, which we constructed according to the WiMedia ECMA-368 standard specifications (ECMA International, 2008). Simulations were done over a UWB channel as described by Molisch et al. (2003), where four separate channel models (CM1-CM4) are available for UWB system modelling, each with arrival rates and decay factors chosen to match a different usage scenario (Foerster, 2002). The four models are as follows,

- CM1: 0–4 m line-of-sight (LOS)
- CM2: 0–4 m non-LOS

- CM3: 4–10 m non-LOS
- CM4: extreme non-LOS multipath channel.

We selected CM2 model for our simulations, since we target high data rates, which are naturally possible to achieve only at short ranges (0−4 m). Also, this model complies with the non-LOS nature of most indoor environments intended for UWB operation. The model is provided with 100 channel realisations that can be found in the report by Foerster (2002). Results shown represent the average of the best 5 channel realisations amongst 20 randomly-selected channel realisations. All PER curves were obtained by averaging PER values over different notch locations.

We assumed also that the receiver is aware of the TN IE employed by the transmitter in all cases. This is a realistic assumption since TN IE is included within beacons that are transmitted using the most robust data rate as explained earlier in Section 2. In addition, although data rate of 400 Mb/s employs DCM scheme for modulation, we assumed QPSK modulation for all data rates studied, in order to provide a common platform for comparing the impact of changing transmission parameters on performance.

Finally, our simulations do not incorporate implementation-related losses such as clipping at the DAC, ADC degradation, clock frequency mismatch, carrier offset recovery, etc. Nevertheless, they incorporate losses due to front-end filtering and channel estimation errors including those due to pilot tone nulling.

5.2 Performance response to increasing notch width

Consumer demand is always targeting higher data rates. However, as data rate get higher, the redundancy added for error correction is correspondingly reduced to maximise throughput. This renders performance more vulnerable to deterioration upon nulling tones. Figure 11 demonstrates the effect of increasing the notch width on the link performance at data rate of 400 Mb/s, which does not employ spreading (see Table 2). Hence, the only error recovery technique available is channel coding, which is a rate 5/8 convolutional code.

Figure 11 Performance of conventional DAA vs. ADD for different notch widths at 400 Mb/s (no spreading)

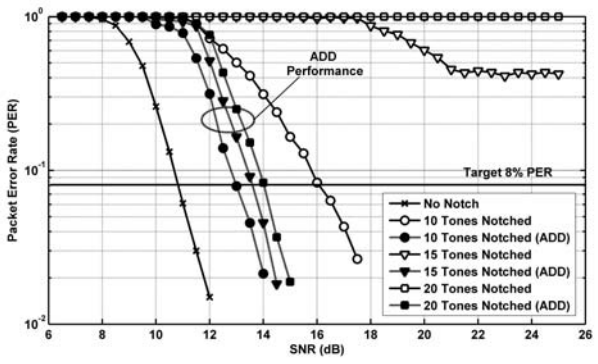

The figure shows PER curves for 10, 15 and 20 nulled tones (notch widths of 41.25, 61.9 and 82.5 out of 1584 MHz), respectively. We can see that the slope of the PER curves decreases as the notch width increases, which implies that, as the slope decreases, larger SNR values are required to reach 8% PER. For ten nulled tones, target PER could be reached at 5 dB increase in SNR. This signifies that, despite the corruption of data carried on the ten nulled tones, the error correction technique (convolutional coding of rate 5/8 in this case) is still capable of recovering corrupted data. On the other hand, for 15 and 20 notched tones, PER reached a phase of saturation after which increasing SNR does not affect performance. This phase is reached when the error correction technique is incapable of recovering the data carried on nulled tones. The reason is that increasing SNR only reduces error probability at the non-notched band, but it does not provide any advantage at the notched band.

On the other hand, when ADD is applied, the PER curves follow almost the same slope as that of the '*no notch*' curve, since nulled tones are not used at all for transmission; and according to (22), HRC theoretically should follow the slope of its standard component code rates, as it is a linear combination of both rates. Degradation introduced by ADD is represented by a horizontal shift, which is referred to the increase in code rate employed, and governed by (24).

The results in Figure 11 imply that high data rates (those do not employ any sort of spreading) are incapable of performing under DAA except for a very small number of nulled tones, else the link is subject to failure. This agrees with the results presented in Mishra et al. (2007) for data rate 480 Mb/s. On the other hand, For ADD, as the number of nulled tones increase, performance degradation in ADD curves is minimal (about 0.4 dB for every additional 5 nulled tones) compared to conventional DAA. Thus, ADD can allow nulling more tones safely with negligible degradation in performance, even for high data rates that lack the advantage of spreading. This advantage is valid as long as the number of nulled data carrying tones is less than or equal to $\delta_{\max}$ (see Table 3). Values of $\delta_{\max}$ can be increased if c_{max} was further increased.

5.3 Impact of employing TDS on performance

Link performance was easily deteriorated at high data rates, as we have seen in the previous section. TDS, which is used in data rates of 106.7, 160 and 200 Mb/s can give a significant performance advantage for a device employing tone nulling. Repeating transmitted symbols can remedy data loss due to nulling at a certain band, as it is retransmitted on the following time slot at a different location of the transmission band. This comes at the price of dividing the transmission data rate by a factor of 2.

Figure 12 compares degradation implied from nulling ten tones in case TDS is applied (rate = 200 Mb/s) vs. TDS not applied (rate = 400 Mb/s). It shows how that, besides the typical improvement in performance represented in the horizontal shift in SNR axis for TDS-applied curves,

applying TDS reduces the degradation in notched-spectrum link performance compared to the case where TDS is not applied. Referring to the fact that TDS repeats transmitted symbols twice, the uncertainty resulting from tone nulling is significantly reduced by the existence of another replica of corrupted data. As a result, degradation is only about 1.5 dB at 200 Mb/s compared to about 5 dB at 400 Mb/s.

Figure 12 Comparison between performance of data rate employing TDS (200 Mb/s) vs. data rate not employing TDS (400 Mb/s) for ten nulled tones

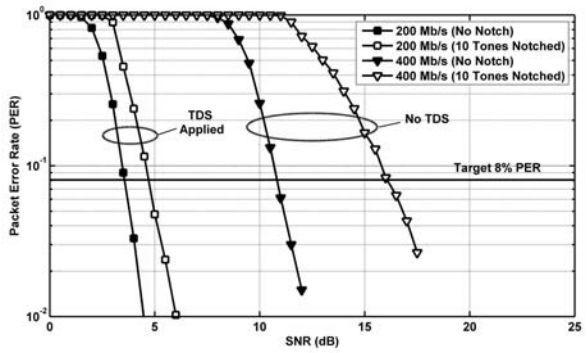

Consequently, it could be concluded that ADD would not consequently provide any significant improvement for rates employing TDS, as performance is expected to be satisfactory with TDS only. This may be true for small numbers of nulled tones, as shown in Figure 13, for 20 nulled tones in TDS mode (data rate 200 Mb/s); ADD does not provide any considerable gain. However, for a larger number of nulled tones, ADD offers about 4 dB gain if 50 tones are nulled. The advantage here comes from the fact that employing ADD allows a UWB device to take full advantage of spreading, although its spectrum is notched, since the notched portion of transmission band is avoided. Consequently, both replicas of OFDM symbol are not corrupted due to the notched portion of the transmitted band. In other words, ADD gives a twofold link enhancement, through protecting transmitted date from being lost, and making full use of spreading.

Figure 13 Impact of employing TDS on gain provided by TDS, for conventional DAA, compared to ADD, data rate = 200 Mb/s

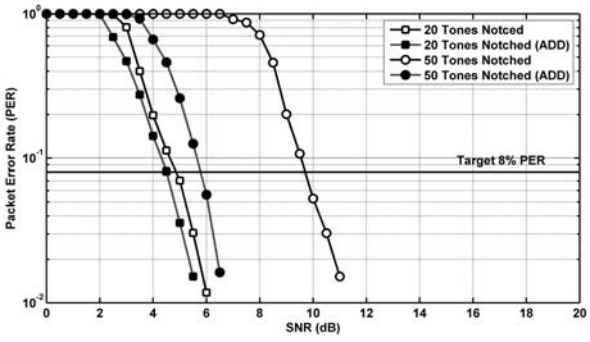

5.4 Impact of transmission mode variation on performance

We mentioned earlier that a UWB transmitter may frequency-hop between one or two or three bands according to its TFC pattern. A device might use different TFCs according to different situations it might face, or because of certain regulatory restrictions. For example, in Table 1, only two bands are allowed to be used in BG1 in Japan, this means that a device transmitting on BG1 in Japan is forced to choose a TFC that hops between two bands. Another example is also BG1 in China, where Table 1 shows that only one band is allocated in this band group. Thus, no hopping will occur in this band. This mode is usually called 'frequency division multiple access (FDMA) mode'.

Figure 14 Impact of transmission mode variation on link performance, for conventional DAA, compared to ADD, notch width = 30 tones at 200 Mb/s

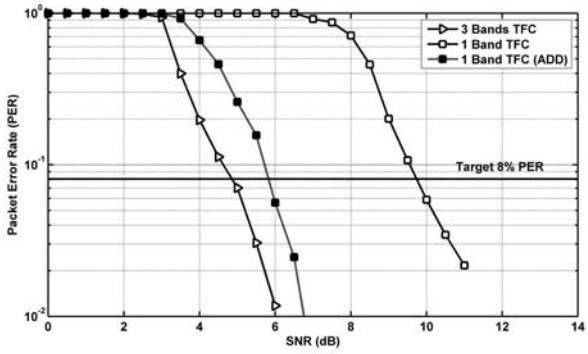

Figure 14 highlights this critical issue, which is how different TFC patterns perform under with nulled tones within its spectrum. The figure compares link performance with 20 nulled tones in case of frequency hopping between 3 bands (Full multi-banding mode) to the case of one band only is used for transmission (FDMA mode) at data rate of 200 Mb/s, which employs TDS. Full multi-banding outperforms FDMA mode with about 5 dB in this case. This can be justified by the following reasons:

1 20 nulled tones represent only 5.2% of the total BW (30 out of 384 tones) in full multi-banding mode. However, in FDMA mode, 20 tones represent about 15.6% (20 out of 128 tones) of total BW.

2 Time domain spreading does not give considerable advantage in FDMA mode, because the spreaded OFDM symbol is sent twice over the same band, and the same notch location, and hence the diversity advantage provided by TDS is reduced, as a portion in both replicas of the transmitted OFDM symbols is corrupted.

Conventional DAA thus does not make full use of TDS, especially in FDMA mode. On the other hand, upon applying ADD, the deterioration in performance caused by switching to FDMA mode is reduced by about 4 dB, as shown in Figure 14, since ADD allows FDMA mode to

make full use of the diversity advantage provided by TDS, as explained earlier. This implies that ADD makes UWB performance almost transparent to different TFCs it might employ.

6 Conclusions

This paper as a whole has focused on the WiMedia MB-OFDM UWB system which is the de facto industry standard for high-rate UWB applications. We presented DAA mechanism as the solution chosen by worldwide regulatory bodies for UWB coexistence issues. DAA was proven in literature − and confirmed in our work− to results in degrading the performance of UWB link. We proposed the ADD technique and showed that it could boost performance significantly in return to minor extensions to the physical layer architecture. The outcomes of this paper can be summarised as follows:

- Enabling a UWB device undergoing DAA mechanism to coexist with larger number of narrowband users by allowing it to notch a larger portion of its bandwidth while maintaining data rate.
- Ability to achieve any code rate with unconventional value through the HRC scheme, using a small set of puncturing patterns.
- Making better use of the diversity advantage provided by spreading, even though numerous portions of transmit spectrum are notched. This could provide about 4 dB gain at 200 Mb/s with 50 notched tones.
- Enabling UWB device to perform efficiently in non-frequency hopping modes, this is particularly desirable in cases where local regulations restrict the use of a single or two bands only in a band group, as in China, Korea and Japan.

Our work can be integrated in the WiMedia UWB physical layer without requiring major modifications, and adds minor complexity to operation. Therefore, it complies with the spirit of the low cost consumer electronics applications intended for UWB. Furthermore, it operates with full transparency to upper layers, since the whole operation can run and be controlled within physical layer.

References

Ahmed, B. and Ramon, M. (2009) 'Coexistence between UWB and other communication systems – tutorial review', *International Journal of Ultra Wideband Communications and Systems*, Vol. 1, No. 1, pp.67–80.

Batra, A. and Balakrishnan, J. (2006) 'Improvements to the multi-band OFDM physical layer', Paper Presented at the *3rd IEEE Consumer Communications and Networking Conference*, Las Vegas, NV, USA, January 8–10.

Batra, A. et al. (2004) 'Multi-band OFDM physical layer proposal for IEEE 802.15 task group 3a', *IEEE P802.15 Working Group for Wireless Personal Area Networks* (*WPANs*), *doc: IEEE P802.15 03/268r4*.

Batra, A., Lingam, S. and Balakrishnan, J. (2006) 'Multi-band OFDM: a cognitive radio for UWB', Paper Presented at the *IEEE International Symposium on Circuits and Systems*, Island of Kos, Greece, May 21–24.

Bocharova, I.E. and Kudryashov, B.D. (1997) 'Rational rate punctured convolutional codes for soft-decision Viterbi decoding', *IEEE Transactions on Information Theory*, Vol. 43, No. 4, pp.1305–1313.

Brandes, S., Cosovic I. and Schnell, M. (2005) 'Reduction of out-of-band radiation in OFDM based overlay systems'. Paper Presented at the *First IEEE International Symposium on New Frontiers in Dynamic Spectrum Access Networks*, Baltimore, MD, USA, November 8–11.

Chiang, J. and Lansford, J. (2005) 'Use of cognitive radio techniques for OFDM ultrawideband coexistence with WiMAX', Paper Presented at the *Texas Wireless Symposium*, Austin, Texas, USA, October 26–28.

Chiani, M. and Giorgetti, A. (2009) 'Coexistence between UWB and narrow-band wireless communication systems', *Proceeding of the IEEE*, Vol. 97, No. 2, pp.231–254.

Clancy, T.C. and Walker, D. (2006) 'Spectrum shaping for interference management in cognitive radio networks', Paper Presented at the *2006 Software Defined Radio Technical Conference and Product Exposition*, Orlando, FL, USA, November 13–17.

Commission of the European Communities (2007) 'Commission decision of 21/II/2007 on allowing the use of radio spectrum for equipment using ultra-wideband technology in harmonised manner in the community', February 21, Brussels.

Duranti, A. et al. (2006) 'Performance evaluation of detect and avoid procedures for improving UWB coexistence with UMTS and WiMax systems', Paper Presented at the *2006 IEEE International Conference on Ultra-Wideband*, Waltham, NA, USA, September 24-27.

ECMA International (2008) *High Rate Ultra Wideband Physical Layer and MAC Standard*, ECMA-368, 3rd ed. December.

Ely, J. et al. (2004) 'UWB EMI to aircraft radios: field evaluation on operational commercial transport airplanes', Paper presented at the *23rd Digital Avionics Systems Conference*, Hudson, OH, USA, October 24–28.

FCC: Federal Communications Commission (2002) 'Revision of part 15 of the commission's rules regarding ultra-wideband transmission systems, first report and order', Washington, DC, ET Docket 98-153, FCC 02-48.

Foerster, J. (2002) 'Channel modeling sub-committee report (final)', *IEEE P802.15- 02/368r5-SG3a*, November.

Kim, C. et al. (2008) 'Policy and technology of dynamic spectrum access in Korea', Paper presented at the *International Conference on Cognitive Radio Oriented Wireless Networks and Communications*, Singapore, May 15–17.

Li, T., Mow, W-H. and Siu, M-H. (2003) 'A joint approach to erasure marking and viterbi decoding for impulsive noise channels', Paper Presented at the *4th IEEE Workshop on Signal Processing: Advances in Wireless Communications*, Rome, Italy, June 15-18.

Liu, K-H et al. (2009) 'Performance analysis of distributed reservation protocol for UWB-based WPAN', *IEEE Transactions on Vehicular Technology*, Vol. 58, No. 2, pp.902–913.

MIC: Ministry of internal Affairs Communications, (2005) 'The report of UWB radio system group', February 2005, Japan.

Mishra et al. (2007) 'Cognitive technology for ultra-wideband/WiMax coexistence', Paper Presented at the *2nd IEEE International Symposium on New Frontiers in Dynamic Spectrum Access Networks*, Dublin, Ireland, April 17–29.

Mishra et al. (2007) 'Detect and avoid: an ultra-wideband/WiMax coexistence mechanism', *IEEE Communications Magazine*, Vol. 45, No. 6, pp.68–75.

Molisch, F., Foerester, J.R. and Pendergrass, M. (2003) 'Channel models for ultra wideband personal area networks', *IEEE Journal of Wireless Communications*. Vol. 10, No. 6, pp.14-21.

Proakis, J. (2001) *Digital Communications*, 4th ed. McGraw-Hill.

Rahim, A., Zeisberg, S. and Finger, A. (2007) 'Coexistence study between UWB and WiMAX at 3.5 GHz band', Paper Presented at the *IEEE International Conference on Ultra-WideBand*, Singapore, September 24-26.

Rateb, A., Syed-Yusof, S. and Fisal, N. (2008) 'Code rata adaptation for mitigating the effects of DAA mechanisms on the performance of UWB systems', Paper Presented at the *2008 IEEE conference on RF and microwaves*, Kuala Lumpur, Malaysia, December, 2–4.

Rateb, A., Syed-Yusof, S. and Fisal, N. (2009) 'Code rate adaptation for efficient bandwidth utilization in ultra-wideband wireless personal area networks', Paper Presented at the *International Conference on Future Networks*, Bangkok, Thailand, March 7–9.

Rateb, A., Syed-Yusof, S. and Fisal, N. (2010) 'Improvement of ultra-wideband link performance over bands requiring interference mitigation in Korea', *ETRI Journal*, February, Vol. 32, No. 1, pp.44–52.

Ross, G.F. (1973) 'Transmission and reception system for generating and receiving base-band duration pulse signals for short base-band pulse communication system', U.S. Patent 3,728,632, Apr 17.

Shi, K., Zhou, Y., Kelleci, B., Fischer, T.W., Serpedin, E. and Karsilayan, A.I. (2007) 'Impacts of narrowband interference on OFDM-UWB receivers: analysis and mitigation', *IEEE Transactions on Signal Processing*, Vol. 55, No. 3, pp.1118–1128.

Snow, C., Lampe, L. and Schober, R. (2006) 'Impact of tone interference on multiband OFDM', Paper presented at the *2006 IEEE International Conference onUltra-Wideband*, Waltham, MA, USA, September 24–27.

Snow, C., Lampe, L. and Schober, R. (2007) 'WiMAX interference to MB-OFDM UWB systems', Paper presented at the *IEEE Pacific Rim Conference on Communications, Computers and Signal Processing*, Victoria, B.C., Canada, August 22–24.

Tang, H. (2005) 'Some physical layer issues of wide-band cognitive radio systems', Paper presented in the *IEEE International Symposium on New Frontiers in Dynamic Spectrum Access Networks*, Baltimore, MD, USA, November 8-11.

WiMedia Alliance (2009) 'Worldwide regulatory chart', available at: http://www.wimedia.org/en/resources/worldwide_regulatory.asp, (accessed on 11/11/2009).

WiMedia Alliance, http://wimedia.org/en/index.asp.

Yamaguchi, H. (2004) 'Active interference cancellation technique for MB-OFDM cognitive radio', Paper Presented at the *34th European Microwave Conference*, Amsterdam, Netherlands, October 14.